Chapter 5

Development of Biophysical Gradient Layers for the LANDFIRE Prototype Project

Lisa Holsinger, Robert E. Keane, Russell Parsons, and Eva Karau

Introduction

Distributions of plant species are generally continuous, gradually changing across landscapes and blending into each other due to the influence of, and interactions between, a complex array of biophysical gradients (Whittaker 1967; 1975). Key biophysical gradients for understanding vegetation distributions include moisture, temperature, evaporative demand, nutrient availability, and solar radiation. Models to predict plant community distributions across landscapes can be developed by identifying the unique set of biophysical gradients that drive the physiological responses of plant species across landscapes (Guissan and Zimmerman 2000). This method of incorporating information about ecological characteristics into analyses of vegetation distribution, termed gradient modeling, is a standard technique for describing ecosystem composition, structure, and function (Gosz 1992; Kessell 1976; Kessell 1979; Whittaker 1973) and has been applied extensively at varying scales, from local to regional (see Keane and others 2002 for a review of gradient modeling applications). The modeling process essentially involves developing empirical relationships between vegetation distributions and geospatial data describing biophysical gradients to enable extrapolation over space. Modeling accuracy becomes substantially improved by incorporating those biophysical gradients that directly affect vegetation dynamics such as temperature, light, and water (Austin 1980, 1985; Austin and Smith 1989; Franklin 1995). Recent efforts have further demonstrated that the accuracy of mapping vegetation and ecological characteristics using remote sensing techniques is greatly improved through the inclusion of biophysical gradient data as predictive variables (Franklin 1995; Keane and others 2002; Ohmann and Gregory 2002; Rollins and others 2004).

The Landscape Fire and Resource Management Planning Tools Prototype Project, or LANDFIRE Prototype Project, was conceived, in part, with the objective of developing methods and procedures for mapping vegetation composition and structure, wildland fuel, and historical conditions at a fine spatial grain (30-m) across the entire United States. This information will facilitate the identification of areas where current vegetation conditions are markedly different from simulated historical conditions (Rollins and others, Ch. 2; Keane and Rollins, Ch. 3). We used a gradient modeling approach to describe vegetation conditions by their potential vegetation type, existing cover type, and existing structural stage (Frescino and Rollins, Ch. 7; Zhu and others, Ch. 8). The overall framework was to use geospatial data representing biophysical gradient variables combined with field-referenced data describing vegetation composition in a classification and regression tree-based approach to map potential vegetation type (Frescino and Rollins, Ch.7) and then incorporate Landsat imagery to map existing vegetation composition, density, and height (Zhu and others, Ch. 8).

We assumed that our accuracy in modeling these vegetation characteristics would be optimized by using biophysical gradient information, which included climatically derived variables related to physiological

In: Rollins, M.G.; Frame, C.K., tech. eds. 2006. The LANDFIRE Prototype Project: nationally consistent and locally relevant geospatial data for wildland fire management. Gen. Tech. Rep. RMRS-GTR-175. Fort Collins: U.S. Department of Agriculture, Forest Service, Rocky Mountain Research Station.

responses of vegetation composition and structure (Austin and Smith 1989). Although geospatial data describing biophysical gradients may exist in certain specific locations, we could not rely on the availability of these data across the nation at spatial scales that met the LANDFIRE design criteria of national consistency (Keane and Rollins, Ch. 3); therefore, we relied on simulation of biophysical gradient data. A number of biogeochemical simulation models and statistical techniques were available to estimate biophysical gradients across spatial domains (Keane and Holsinger 2006; Kessell 1979; Thornton and White 2000; Thornton 1998; White and others 1997). We chose to use the simulation model WXFIRE to develop biophysical gradient data because the model represents a balance of sophistication and computational efficiency. WXFIRE simulates a suite of gradients proven to describe both biotic and abiotic characteristics and processes that directly influence ecosystem composition, structure, and function (Keane and others 2002; Keane and Holsinger 2006; Rollins and others 2004).

We implemented the LANDFIRE methods in two large prototype areas to test the feasibility of national application of the LANDFIRE design criteria and guidelines. The study areas were based on mapping zones developed for the USGS Multi-Resolution Land Characteristics (MRLC) 2001 project (landcover.usgs.gov/index.asp). We first applied our methods to Zone 16, located in central Utah, and then, based on lessons learned, applied refined methods in Zone 19, located in the northern Rocky Mountains (see fig. 1 in Rollins and others, Ch. 2). Most of the biophysical gradient layers were derived using the WXFIRE simulation model implemented with data from the DAYMET weather database, which comprises daily weather data across the conterminous United States (Thornton and others 1997; Thornton and others 2002; Thornton and Running 1999). We also acquired or derived ancillary geospatial data for use as predictors in vegetation gradient modeling (for example, topography from the National Elevation Database). In this chapter, we describe our methods for creating the biophysical gradient layers, including the development of WXFIRE input and simulation procedures. We also describe the resulting biophysical gradient layers used for mapping potential vegetation type, existing vegetation, structural stage, and canopy fuel. (Frescino and Rollins, Ch. 7; Zhu and others, Ch. 8; Keane and others, Ch. 12). Further, the LANDFIRE biophysical gradient layers could potentially be applied in other land management purposes, such as hydrological studies or quantification of thermal cover for wildlife.

In the process of developing these protocols for the LANDFIRE Prototype Project, we identified numerous improvements that could be made to our methods, and we outlined a set of recommendations for future development of biophysical gradient layers. Hence, the methods described here do not necessarily reflect the protocols followed by LANDFIRE National (Rollins and others, Ch. 2).

Methods

The LANDFIRE Prototype Project involved many sequential steps, intermediate products, and interdependent processes. Please see appendix 2-A in Rollins and others, Ch. 2 for a detailed outline of the procedures followed to create the entire suite of LANDFIRE Prototype products. This chapter focuses specifically on the procedure followed in developing biophysical gradients, which served as spatial predictors in mapping models for nearly all mapping tasks in the LANDFIRE Prototype Project.

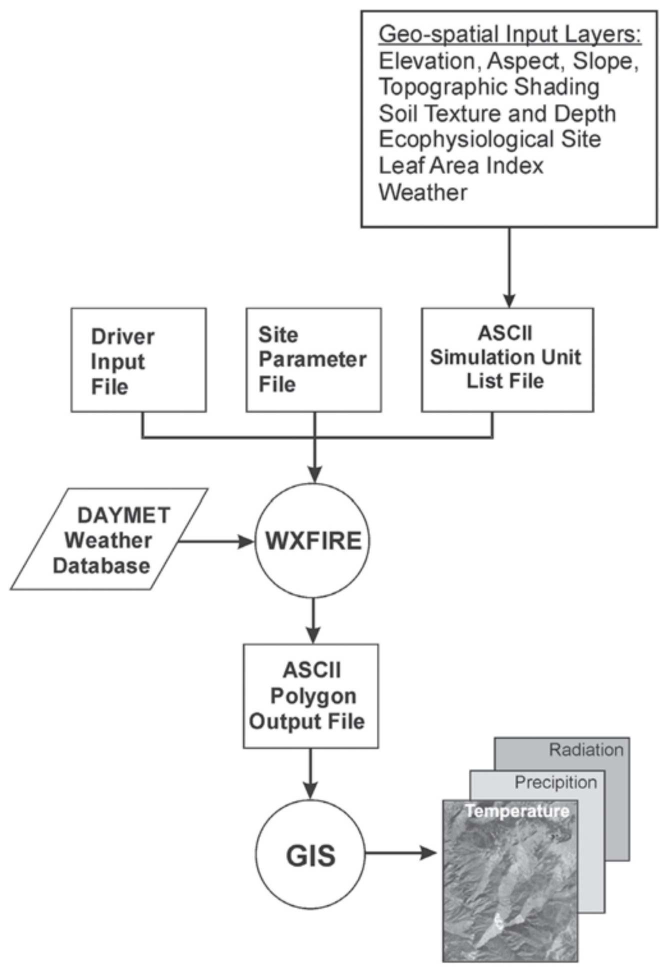

Figure 1—The flow and component diagram for the WXFIRE program.

Spatial Units used in Modeling

We applied numerous spatial units in creating biophysical gradients, ranging in spatial extent from large, regional mapping zones to simulation units of intermediate size to 30-m pixels. These various spatial units used in the WXFIRE modeling process require some initial explanation here for clarity. Detailed descriptions are provided in the following sections. At the broadest scale, we divided the U.S. into regional mapping zones ranging in size from five to fifteen million ha, and we applied our protocols to mapping zones 16 and 19, which were six and ten million ha, respectively. Next, the mapping zones were divided into simulation units representing unique environmental conditions for the purposes of estimating biophysical gradients using the WXFIRE simulation model. Simulation units were derived by combining the key spatial WXFIRE inputs such as soils data and topography. Simulation units ranged in pixel size from 0.09-ha to 575-ha in Zone 16 and 0.09-ha to 144-ha in Zone 19.

Another spatial unit was developed for describing biophysical settings. The WXFIRE model required a set of data representing specific ecophysiological parameters for landscapes (table 1). These parameters could have been included in the development of simulation units because they describe unique environmental conditions. However, WXFIRE requires so many parameters (45) that, for expediency in model simulations, those ecophysiological parameters are simply assumed to be relatively homogenous over fairly broad areas or across spatial units termed ecophysiological 'sites' (Keane and Holsinger 2006). For example, albedo is an ecophysiological parameter required by the WXFIRE model, and it should be relatively constant across many simulation units in a landscape for many days of the year. WXFIRE runs far more efficiently by assigning albedo (along with the other 44 ecophysiological parameters) to a site, rather than determining unique parameter values for every simulation unit. Typically, one site encompasses many simulation units. As such, we identified ecophysiological sites across our mapping zones and then assigned unique values to all ecophysiological parameters for each site. The sites ranged in size from 6.25 to 4.6 million ha in Zone 16 and 6.25 to 2.2 million ha in Zone 19.

Overview of the Modeling Process

We developed biophysical gradient layers in several steps for each mapping zone (fig. 1). First, we collected and modified various topographic, soil, weather, and vegetation-related layers and grouped the values in these layers into classes to improve the computational efficiency of the model. We then partitioned each mapping zone into simulation units by spatially combining all of the classified input layers (fig. 1; table 2). That is, each unique spatial combination of the values for the input layers identified a distinct simulation unit. Next, we assembled the three input files needed to run WXFIRE, including: 1) the simulation unit file containing soil, topographic, weather, and vegetation-related data for all the simulation units in a mapping zone (*simulation unit list file*) (fig. 2); 2) a file specifying general simulation options (*driver file*), such as time frames for summarizing data; and 3) a parameter file describing the ecophysiological site conditions (*site file*). We then ran WXFIRE simulations and produced tabular data of biophysical gradients for each simulation unit. Finally, we linked the tabular data to the spatial layer of simulation units to create geospatial biophysical gradient layers for each mapping zone. In the following sections, we briefly discuss the WXFIRE and DAYMET computer models used to generate biophysical gradients and then cover in detail our process for developing those layers.

Computer Models for Developing Biophysical Gradient Layers

The WXFIRE model was developed with the goal of employing standardized and repeatable modeling methods to derive spatially explicit, climate-based biophysical gradients for predictions of landscape characteristics related to ecosystem management (Keane and others 2002; Rollins and others 2004). Keane and others' (2002) first model, WXGMRS, was built for a spatially explicit gradient modeling application called the Landscape Ecosystem Inventory System. The next generation of this model, WXFIRE, was used for creating biophysical gradient layers in the LANDFIRE Prototype Project (Keane and Holsinger 2006). The WXFIRE model is designed for simulating biophysical gradient data at any geographic extent or spatial resolution using spatial data layers of daily weather, soils, topography, leaf area index, and a suite of ecophysiological parameters. The WXFIRE model produces a broad array of biophysical gradients that can be categorized into two general types: 1) weather and climate variables and 2) ecosystem variables. The weather variables describe daily weather conditions (maximum daily temperature), whereas the climate variables summarize weather conditions over broader temporal periods (decades) to describe the climatic regime of the study area (for example, solar radiation flux to the ground). The ecosystem variables describe how climate variables interact with vegetation.

Table 1—Parameters required in the ecophysiological site input file for WXFIRE (Keane and Holsinger 2006) for a montane site (1,800 – 2,700 m) in Zone 16.

Ecophysiological parameter	Units	Value
Julian date of start of pre-greenup period	Jday	135
Julian date of initiation of greenup period	Jday	149
Julian date of end of greenup period	Jday	190
Julian date indicating live fuels are frozen	Jday	300
LAI of the site in m2/m2	m^2/m^2	2.5
LAI conversion factor	index	3.54
Extinction coefficient	index	0.48
Rainfall interception coefficient	index	0.0005
Average site albedo (dim) for climax stand	index	0.18
Leaf water potential at stomatal opening	-MPa	-0.5
Leaf water potential at stomatal closure	-MPa	-1.65
Min vapor pressure deficit stomatal opening	Pa	500.0
Max vapor pressure deficit stomatal closure	Pa	4100.0
Maximum canopy conductance	m sec^{-1}	0.0065
Leaf boundary layer conductance	m sec^{-1}	0.0865
Leaf cuticular conductance	m sec^{-1}	0.00001
Maximum live foliar moisture content	percent	200.0
Minimum live foliar moisture conten	percentt	80.0
DBH of reference tree	cm	50.0
Bark conversion factor	cm bark/cm dbh	0.05
Live crown ratio	percent	50.0
Tree height	meters	25.0
Initial fuel moisture content - 1-hr woody	percent	20.0
Initial fuel moisture content - 10-hr woody	percent	20.0
Initial fuel moisture content - 100-hr woody	percent	25.0
Initial fuel moisture content - 1000-hr woody	percent	30.0
Initial fuel moisture content - live foliage	percent	120.0
Initial fuel moisture content - litter	percent	100.0
Initial fuel moisture content - duf	percent	150.0
Initial fuel moisture content - shrub	percent	100.0
Initial fuel moisture content - herb	percent	140.0
FOFEM cover type ID number	code	11
NFDRS fuel model number (a=1...z=26)	code	12
FBFM ID number from Anderson et al. (1982)	code	10
FLC fuel loading model ID number	code	122
Elevation of site	meters	2500.0
Aspect of site	degrees	180.0
Slope of site	percent	10.0
Latitude of site	decimal-deg	45.12345
Longitude of site	decimal-deg	120.12345
Depth of soil defining free rooting zone	meters	1.0
Percent sand in soil profile in FRZ	percent	50.0
Percent silt in soil profile in FRZ	percent	30.0
Percent clay in soil profile in FRZ	percent	20.0
Average wind speed	m sec^{-1}	10.0
Topographic shading reduction factor	m sec^{-1}	1.00

Table 2—Spatial input data for developing simulation units for the WXFIRE simulation model.

Layer name	Description	Data scale or resolution	Source
Aspect	Direction of exposure in azimuths	30-m pixel	Derived (ESRI 2002)
DAYMET	Daily weather data	1-km pixel	Derived (Nemani et al. 1993)
Elevation	Digital Elevation Model (DEM) (m)	30-m pixel	Thornton et al. 1997
LAI	Leaf area index	30-m pixel	USGS 2002
Percent sand	Percent of sand in soil	1:250,000	SCS 1991
Percent silt	Percent of silt in soil	1:250,000	SCS 1991
Percent clay	Percent of clay in soil	1:250,000	SCS 1991
Shading	Ecophysiological site conditions	30-m pixel	Derived (ESRI 2002)
Site	Topographic shade index	30-m pixel	DEM & USGS NLCD
Slope	Slope derived from DEM in percent	30-m pixel	Derived (ESRI 2002)
Soil depth	Soil depth to bedrock (cm)	30-m pixel	Derived (Zheng et al. 1996)

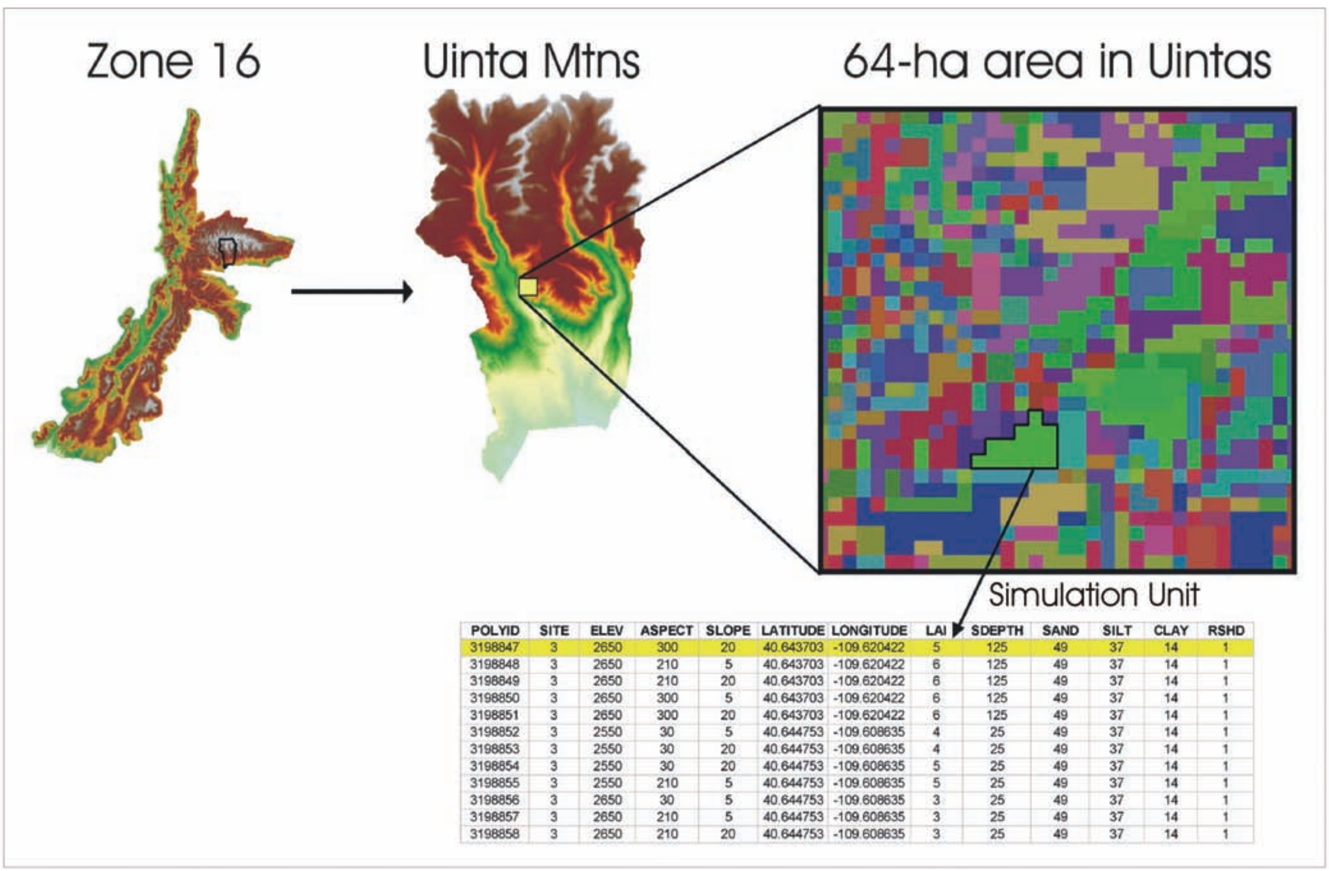

POLYID	SITE	ELEV	ASPECT	SLOPE	LATITUDE	LONGITUDE	LAI	SDEPTH	SAND	SILT	CLAY	RSHD
3198847	3	2650	300	20	40.643703	-109.620422	5	125	49	37	14	1
3198848	3	2650	210	5	40.643703	-109.620422	6	125	49	37	14	1
3198849	3	2650	210	20	40.643703	-109.620422	6	125	49	37	14	1
3198850	3	2650	300	5	40.643703	-109.620422	6	125	49	37	14	1
3198851	3	2650	300	20	40.643703	-109.620422	6	125	49	37	14	1
3198852	3	2550	30	5	40.644753	-109.608635	4	25	49	37	14	1
3198853	3	2550	30	20	40.644753	-109.608635	4	25	49	37	14	1
3198854	3	2550	30	20	40.644753	-109.608635	5	25	49	37	14	1
3198855	3	2550	210	5	40.644753	-109.608635	5	25	49	37	14	1
3198856	3	2650	30	5	40.644753	-109.608635	3	25	49	37	14	1
3198857	3	2650	210	5	40.644753	-109.608635	3	25	49	37	14	1
3198858	3	2650	210	20	40.644753	-109.608635	3	25	49	37	14	1

Figure 2—Example of WXFIRE simulation units for a small landscape in the Uinta mountains of Zone 16 and associated WXFIRE tabular input, including: simulation unit identifier (POLYID), ecophysiological site (SITE), elevation (ELEV), aspect, slope, geographic coordinates for weather, LAI, soil depth (SDEPTH), percents sand, silt and clay, and topographic shading (RSHD).

For example, actual evapotranspiration can describe the moisture available for vegetation development much better than average annual precipitation because it integrates phenology, temperature, and soil water dynamics. Keane and Holsinger (2006) provide extensive documentation of WXFIRE, including structure and formats of all input and output files, complete descriptions of all model algorithms, and guides on preparing and executing the program.

DAYMET is a computer model that extrapolates daily spatial surfaces of temperature, precipitation, radiation, and vapor pressure deficit across large regions (Thornton and others 1997, Thornton and others 2002; Thornton and Running 1999). The DAYMET model requires digital elevation data, minimum and maximum temperature, and precipitation from ground-based meteorological stations. The DAYMET model extrapolates station-based weather data across broad regions using a spatial convolution method with a truncated Gaussian weighting filter (Thornton and others 2002). The DAYMET weather database was compiled for the entire nation using over 1,500 weather stations and served as a key input to the WXFIRE model. The DAYMET weather database contains gridded 1-km resolution daily data for daily minimum and maximum temperature (°C), precipitation (cm), solar radiation (W m^{-2}), and vapor pressure deficit (percent) from 1980 to 1997. At this time, the DAYMET model is unique in its ability to provide data at a temporal (18 years of daily data) and spatial (1-km) resolution across the conterminous U.S.

Input Layers for Developing WXFIRE Simulation Units

This section details the process used to create the spatial data input layers required by WXFIRE (fig. 1). Specifically, we describe the procedures used to synthesize information from existing spatial data layers, including a suite of terrain-related layers and layers of soils, leaf area index, weather and ecophysiological site. These input layers were subsequently used to develop simulation units and to compute the attributes for each simulation unit required as input into the WXFIRE model (table 2).

Developing terrain-related input layers—We classified continuous data describing slope, aspect, and topographic shading as input to the WXFIRE model. Each layer was derived using digital elevation models (DEM) from the National Elevation Database (http://edc.usgs.gov/products/elevation/ned.html) and standard algorithms for deriving topographic derivatives. We calculated slope as the rate of maximum change in a DEM from each cell relative to its neighbors using a 3x3 grid cell neighborhood and an average maximum technique (Burrough 1986; ESRI 2002). Aspect was calculated by identifying the direction of maximum rate of change in a DEM between each cell and its neighbors (ESRI 2002). The topographic shading layer represented how direct radiation to a landscape area was attenuated by the surrounding high topography. The topographic shading layer was created by developing a shaded relief grid from a DEM, projecting an artificial light source onto the surface, and determining reflectance values. Solar azimuth and altitude for the sun's position were required inputs for this process. We calculated azimuth and altitude using the National Oceanographic and Atmospheric Association Solar Position calculator (http://www.srrb.noaa.gov/highlights/sunrise/azel.html, assuming the summer solstice as the date and using the center coordinates for each mapping zone.

Developing soil-related input layers—WXFIRE required soil texture (percent) and soil depth (m) as input for each simulation unit. Soil texture was derived using the State Soil Geographic (STATSGO) geo-spatial data, which is composed of digitized polygons from 1:250,000 scale state soil maps (Natural Resources Conservation Service or NRCS 1995a). We explored the finer-scale Soil Survey Geographic (SSURGO) data but found that SSURGO has incomplete coverage across the two prototype regions and would not provide sufficient soils information for the national LANDFIRE mapping effort (NRCS 1995b). The STATSGO data structure consists of soil polygons, where each polygon has associated descriptions of soil sequence and soil layers in tabular format. Soil sequence represents the dominant kinds of soils (up to three taxonomic classes) contained in a polygon. Geographic locations for these soil sequences are not available but are instead represented as percents for each soil polygon. Soil information for the STATSGO polygons includes vertical composition (soil horizons) (up to six layers) for each soil sequence (soil taxonomic class).

The WXFIRE model required that soil texture be described in terms of percent sand, silt, and clay (Keane and Holsinger 2006). These data are not directly defined in the STATSGO attribute list but can be extracted from the database based on variables describing the percent by weight of particles passing through various sieve sizes and percent clay content (Thornton and White 2000). We first calculated four soil textures from the STATSGO database, including coarse fragment content and percent sand, silt, and clay. We computed the

Table 3—Soil texture calculations based on STATSGO attributes that describe the percent by weight of particles passing through various sieve sizes and percent clay content (Thornton and White 1999).

Soil texture	Equation using STATSGO attributes
Coarse fragment content	Percent passing No. 10 sieve
Percent sand	Percent passing No. 10 sieve – Percent passing No. 200 sieve
Percent clay	Percent clay weighted by percent passing No. 200 sieve
Percent silt	Percent passing No. 200 sieve – (percent clay – percent passing No. 10 sieve)

four soil textures according to criteria for soil particle variables, described in table 3, using a script for SAS software (SAS System for Windows 2001). STATSGO data provides only high and low values for these attributes by soil sequence and layer. We calculated an average for each of the soil textures, for example, percent sand = (No. 10 sieve high + No. 10 sieve low) / 2 – (No. 200 sieve high + No. 200 sieve low) / 2, and weighted the STATSGO variables by the layers' depths and by the aerial extent of sequences within STATSGO polygons. Since the WXFIRE model requires measures of percent sand, silt, and clay only, we removed the coarse fragment proportion from the composition of soil textures and rescaled the sand, silt, and clay components to comprise 100 percent of soil texture estimates. Our final results from this analysis were estimates of percent sand, silt, and clay for each of the STATSGO polygons in a mapping zone.

The soil depth layer was also derived using STATSGO data, but we modeled soil depth to a higher resolution using DEM data and hydrologic modeling. For this process, we first extracted the maximum depth per soil sequence from the STATSGO database and weighted these values by their aerial extent to calculate a maximum soil depth per polygon. We then calculated a topographic convergence index (TCI) for each pixel using the following relationship provided by Beven and Kirkby (1979):

$$TCI = \ln\left(\frac{a}{\tan B}\right)$$

where a is the upslope area (m^2) draining past a certain point per unit width of slope and is calculated by accumulating the weight for all cells that flow into each down-slope cell (ESRI 2002; Jenson and Domingue 1988; Tarboton and others 1991) and B is the local surface slope angle (degrees) calculated from a 3x3 grid cell neighborhood using an average maximum technique (Burrough 1986; ESRI 2002). Using methods developed by Zheng and others (1996), we integrated the STATSGO maximum depth layer (STATGO Max Depth) and TCI data to calculate a soil depth value for each pixel using scalars to adjust for skewed TCI distributions as follows:

$$\text{Soil depth} = \{M_1, M_2\} * TCI$$

where M_1 is the scalar used if a pixel's TCI value was less than or equal to its mean across a mapping zone and was calculated by:

$$M_1 = \frac{\text{Ave. Max. Depth}}{0.5 * (LN_{mo} + LN_{me})}$$

where Ave. Max. Depth is the mean value of the STATSGO maximum depth layer across each mapping zone, and LN_{mo} and LN_{me} are mode and mean values for the natural log of TCI. M_2 is the scalar used if a pixel's TCI value is greater than or equal to its mean across a mapping zone and is calculated by:

$$M_2 = \frac{\text{Max. Depth}}{LN_{\max}}$$

where Max Depth is the STATSGO maximum depth layer for each polygon and $LN_{\max}$ is the maximum natural log of TCI.

For Zone 19, we revised this process to improve data resolution by including slope in calculations of soil texture and depth. The STATSGO database provides high and low slope values for each STATSGO polygon. We calculated an average slope and classified the average slope into four classes: (1) ≤4 percent; (2) >4 percent and ≤8 percent; (3) >8 percent and ≤15 percent; and (4) >15 percent (N. Bliss, personal communication). We extracted the soil texture and soil depth variables by these four slope classes from the STATSGO database. We used the slope geospatial layer (percent) previously described and then classified slope into the above four classes. We partitioned the STATSGO polygons by the classified slope layer and linked this spatial layer with the STATSGO variables of soil texture and depth by slope. For the final soil depth layer, we followed with the process described above for integrating STATSGO maximum soil depth with TCI to obtain soil depth values for each pixel. The final products were soil textures and soil depth—with improved resolution by incorporating slope into calculations. Note, improving the soil layers' resolution also contributed to a large increase in the number of records in the simulation unit file for Zone 19 from that of Zone 16.

Developing leaf area index and weather input layers—We generated leaf area index (LAI) from Landsat imagery (30-m pixel resolution) for leaf-on reflectance based on methods developed by Nemani and others (1993). We first calculated a corrected normalized difference vegetation index (NDVI) as follows:

$$NDVI_c = \left(\frac{NIR - RED}{NIR + RED}\right) * \left(1 - \frac{MIR - MIR_{\min}}{MIR_{\max} - MIR_{\min}}\right)$$

where NIR is near infrared (band 4), RED is infrared (band 3), MIR is mid-infrared (band 5), MIR_{min} is the minimum value in mid-infrared band in an open canopy, and MIR_{max} is the maximum value in the mid-infrared band in a closed canopy. We then converted the $NDVI_c$ layer to LAI according to the following equation:

$$LAI = \frac{\ln(0.7 - NDVIc)}{-0.7}$$

Developing the ecophysiological site input layer—For Zone 16, we delineated ecophysiological sites by partitioning the landscape by elevational breaks corresponding to major vegetation changes (for example, landscapes dominated by pinyon pine vs. Douglas-fir). The four sites in Zone 16 included:

Site 1 – Mohave (0 to 1,200 m mean sea level),
Site 2 – Sagebrush (1,200 to 1,800 m MSL),
Site 3 – Montane (1,800 to 2,700 m MSL), and
Site 4 – Subalpine (2,700+ m MSL).

We assigned values to the sets of ecophysiological variables for each site based on previous synthesis efforts (Korol 2001; Hessl and others 2004; White and others 2000). Table 1 shows the ecophysiological parameters and associated values for the Montane site in Zone 16.

For Zone 19, we used a less subjective approach where we developed sites using the U.S. Geological Service/U.S. Environmental Protection Agency National Land Cover Database (http://edcwww.cr.usgs.gov/programs/lccp/natllandcover) and biome types described for national-level ecosystem simulation (Thornton 1998). The National Land Cover Database contains 21 broad cover types, and we summarized these cover types into five general plant functional types and one non-vegetated class: water/barren (table 4). Each of these plant functional types represented a site, and we assigned a set

Table 4—Changes made to National Land Cover Database (NLCD) land cover class definitions for the LANDFIRE site map.

NLCD land cover class	LANDFIRE plant functional types
Open water	Water/barren
Perennial ice/snow	Water/barren
Bare rock/sand/clay	Water/barren
Quarries/strip mines/gravel pits	Water/barren
Transitional	Closest natural vegetation
Low intensity residential	Closest natural vegetation
High intensity residential	Closest natural vegetation
Commercial/industrial/transportation	Closest natural vegetation
Deciduous forest	Deciduous broadleaf forest
Evergreen forest	Evergreen needleleaf forest
Mixed forest	Majority of surrounding deciduous broadleaf forest or evergreen needleleaf forest
Orchards/vineyards/other	Deciduous broadleaf forest
Shrubland	Shrub
Grasslands/herbaceous	Grass
Pasture/hay	Grass
Row crops	Grass
Small grains	Grass
Fallow	Grass
Urban/recreational grasses	Grass
Woody wetlands	Deciduous broadleaf forest
Emergent herbaceous wetlands	Grass

of ecophysiological parameters to each site. The five main plant functional types were C3-grass, evergreen needle leaf forest, deciduous broadleaf forest, shrub, and barren/water. Areas classified as human development, such as urban and agriculture, were assigned a cover type based on the dominant cover type in neighboring pixels. Similarly, areas classified as mixed forest were recoded to either evergreen needle leaf forest or deciduous broadleaf forest based on the dominant forest type in surrounding pixels.

Development of WXFIRE Simulation Units and Model Input Files

Simulation units were developed by combining all 11 spatial data layers described above and detailed in table 2. Ideally (given the available data) we would have combined all input layers for every 30-m pixel to obtain the best resolution possible in the biophysical gradient layers. However, the LANDFIRE prototype mapping zones were very large and would have required the simulation of 284 million records for Zone 16 and 289 million records for Zone 19. Our computer resources were insufficient to process this amount of data in a timely manner. Instead, we reduced the data sets to 10 million and 26 million records for mapping zones 16 and 19, respectively, by classifying input layers to a coarser attribute measurement resolution. That is, we classified spatial layers so that their measurement increments were in broader ranges. Table 5 shows the classification scheme for each of the terrain, soil depth, and LAI layers. For example, slope was grouped into three classes of low, moderate, and high slope. Note that the soil texture layers (sand, silt, and clay) were already at a coarse spatial resolution, so we maintained them in their original form (1:250,000 scale) and did not summarize to a broader attribute measurement resolution.

To create the simulation units for executing WXFIRE, we combined the classified input layers (terrain, soil depth, LAI) with ecophysiological site, soil texture and weather layers such that each unique combination formed one simulation unit. Prior to combining these layers, we re-sampled all input layers to a 25-m pixel size such that each layer nested within the 1-km DAYMET weather data layer. Accordingly, each simulation unit was geo-referenced at a 25-m pixel size and had a series of associated input data. Figure 2 provides an example of WXFIRE simulation units developed for a landscape in the Uinta Mountains of Zone 16. As input to the WXFIRE model, we created an ASCII simulation unit list file that contained records for all the simulation units in a mapping zone along with their associated ecophysiological site identifiers, terrain data, geographic coordinates for weather (latitude and longitude), LAI, and soil values.

WXFIRE Model Simulation and Development of Biophysical Gradient Layers

Using the various input files, the WXFIRE model calculated a series of biophysical gradients for each simulation unit and output the results to ASCII files. We linked each record in the ASCII output files to their corresponding simulation units to create geospatial data representing the biophysical gradients output from WXFIRE. We implemented the WXFIRE model using average annual time frames to consistently measure biophysical gradients across large regions that may have variable growing seasons and to match temporal periods commonly used in other gradient modeling analyses (Waring and Running 1998).

In the initial WXFIRE runs, we retrieved the DAYMET weather data in the model simulations in its native 1-km format in an effort to maximize model efficiency. However, we discovered a strong gridded pattern in the biophysical gradient layers—a direct artifact of the coarsely gridded DAYMET weather maps (fig. 3A). We revised the WXFIRE program to scale the temperature and precipitation maps to a finer resolution using a moving window technique to calculate dynamic lapse rates (fig. 3B) (Keane and Holsinger 2006). The

Table 5—Methods used for classifying input layers to coarser attribute measurement resolution, implemented to reduce the number of input records and computer processing time.

Input layer	Classification method	Number of categories
Elevation	100-m intervals	30+
Aspect	SW (165° to 255°; NW (255° to 345°); NE (345° to 75°); SE (75° to 165°)	4
Slope	Low (<10%); moderate (10% to 30%) and high (≥ 30%)	3
Topographic shading index	Every 0.25 (index)	4
Soil depth	0.5-meter classes	4
LAI	1.0 LAI intervals	9

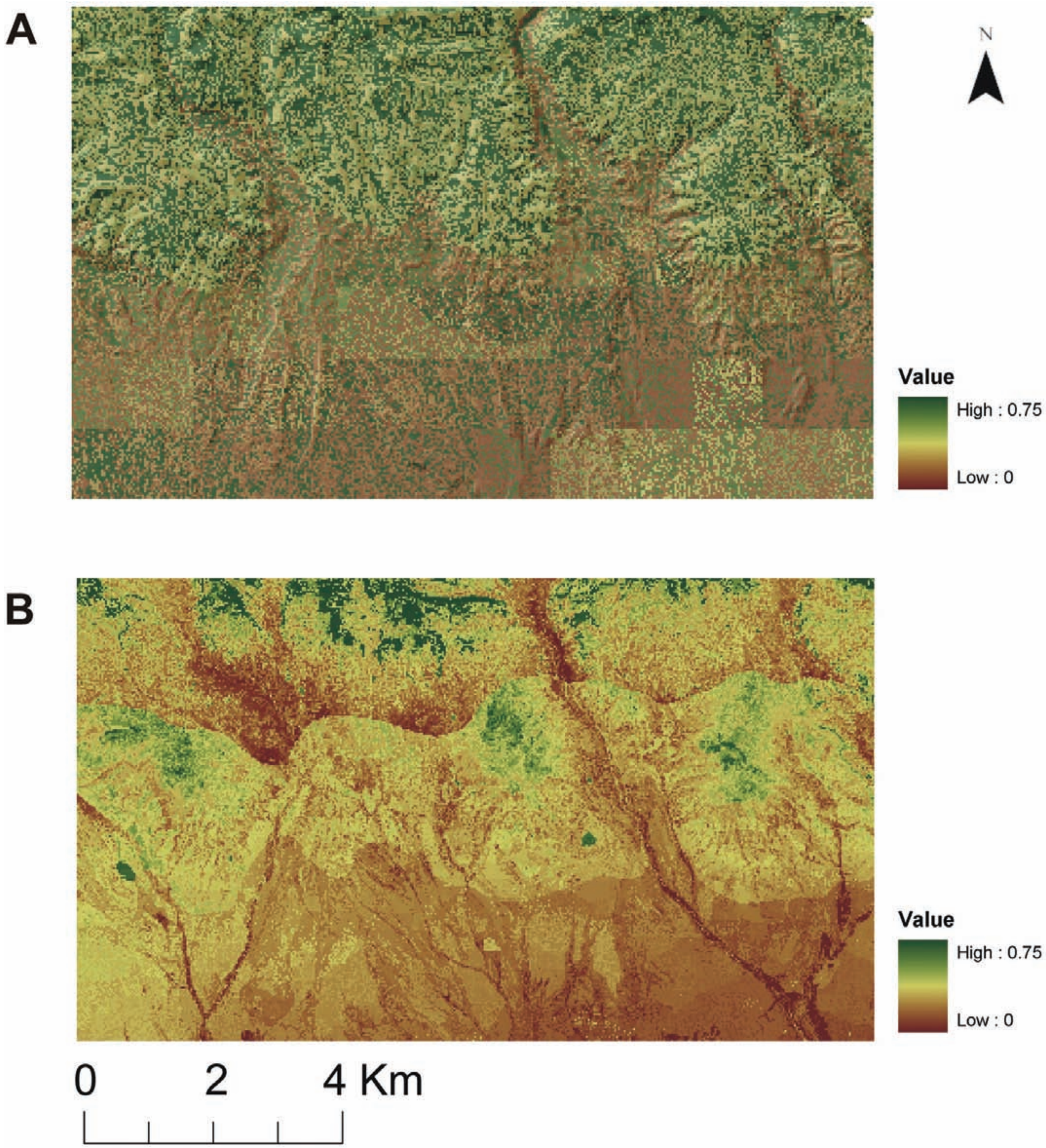

Figure 3—The biophysical gradient soil water fraction for an area in the Uinta mountains where: (A) shows results from initial model run using a static lapse rate calculation (the 1-km DAYMET footprint is particularly evident in southern area); and (B) shows final model run using dynamic lapse rates to scale down weather maps. Use of the dynamic lapse rate dramatically reduced the 1-km DAYMET footprint.

lapse rates were incorporated into linear regressions that adjusted the weather based on the difference in elevation between the coarse-scale DAYMET DEM and the elevation of the simulation unit. Solar radiation was also scaled to the simulation unit using geometric relationships of aspect and slope to sun zenith and azimuth angles (Keane and Holsinger 2006). We used the adiabatic lapse rate correction and the solar radiation adjustment in WXFIRE model runs for both mapping zones to minimize the DAYMET 1-km footprint pattern in output data layers, minimally affecting the efficiency of our model simulations and computational capacity.

Additional Topographic Layers for Gradient Modeling

Additional terrain-related layers were created as predictive layers for developing potential vegetation type, cover type, structural stage, and canopy fuel maps (Frescino and Rollins, Ch.7; Zhu and others, Ch. 8; Keane and others, Ch. 12). Although not part of WXFIRE input or output, we mention these layers in this chapter because they were important biophysical gradients for subsequent mapping applications. One of the terrain-related layers was topographic position index, which describes the exposure of a location in space compared to the surrounding terrain. Positive values expressed ridges or exposed sites, while negative values described sinks, gullies, valleys, or toe slopes. The topographic position index layer was developed using a moving window to describe relative location on a slope (Z. Zhang, personal communication). A topographic relative moisture index layer was developed to describe potential moisture conditions by combining relative slope position, slope configuration, slope steepness, and slope-aspect into a single scalar value based on methods defined by Haplin (1999) and Parker (1982). Finally, a landform layer was created based on reclassifying the topographic relative moisture index and slope. The landform layer described physiographic features such as valley flats, hills, and steep mountain slopes formed by erosion, sedimentation, mass movement, or glaciation (Neufeldt and Guralnik 1988).

Results and Discussion

Demonstration of Biophysical Gradient Layers

We developed thirty-one biophysical gradient layers from WXFIRE simulations to describe weather and climate variables and ecosystem variables (table 6). We created seven additional biophysical gradient layers describing topographic and soil conditions for use in subsequent vegetation and wildland fuel mapping (table 6). The mean, standard deviations, and ranges for each of the biophysical gradient variables in each mapping zone are presented in table 7.

Due to the large number of biophysical gradient layers that can be created by WXFIRE, we present only maps of a subset of the two variable types developed by WXFIRE: weather/climate variables and ecosystem variables. Average annual precipitation (cm) was an important weather/climate variable because it directly influences plant productivity and limits vegetation distributions (fig. 4). Another key weather/climate variable was degree-days, which reflects the heat load to a simulation unit (fig. 5). Potential evapotranspiration (kg H_2O yr^{-1}) is an example of an ecosystem variable modeled in WXFIRE (fig. 6). Potential evapotranspiration integrates temperature, precipitation, radiation, and relative humidity to estimate the maximum evapotranspiration through a vegetated surface. To better demonstrate the spatial patterns in the biophysical gradients, we also present a close-up view of important WXFIRE layers used in predicting potential vegetation type for forested areas of Zone 16 (fig. 7).

Limitations in Developing Biophysical Gradient Layers

The suite of biophysical gradient layers developed for the LANDFIRE Prototype Project must be considered in light of the limitations inherent to the simulation modeling process. Simulation modeling using WXFIRE was based on a set of algorithms that simplify and synthesize correlative relationships and mechanistic understandings of biophysical gradient variables (Keane and Holsinger 2006). The resulting geospatial data do not reflect direct and accurate measurements, but rather approximations of environmental conditions and ecosystem characteristics as they fluctuate across broad landscapes. Specifically, biophysical data developed using simulation modeling demonstrate the transition of biophysical gradients, emphasizing relative differences across large areas. In any given location, estimates for any one of the WXFIRE variables may not be particularly accurate; however, estimates will be consistently measured with high precision across landscapes. Care must therefore be taken to limit mapping applications to relative comparisons of variables across large landscapes and to forego expectation of spatial accuracy at any specific location. Keane and Holsinger (2006) present a detailed accuracy assessment of several WXFIRE weather outputs for several

Table 6—Biophysical gradients developed for the LANDFIRE Prototype Project, including weather, climate, and ecosystem variables simulated by the WXFIRE model and additional geographic variables.

Description	Biological significance
	WXFIRE weather and climate variables
Maximum daily temperature (°C)	Affects evapotranspiration and productivity
Minimum daily temperature (°C)	Limiting factor for plant tolerance
Precipitation (cm)	Directly affects productivity; limiting factor at lowest extreme
Average daily temperature (°C)	Affects evapotranspiration and productivity
Daytime daily temperature (°C)	Determines daily photosynthesis and respiration
Nighttime daily temperature (°C)	Important for dark respiration
Soil temperature (°C)	Affects water availability, soil respiration, nutrient availability
Relative humidity (%)	Determines photosynthesis and evapotranspiration rates
Total solar radiation (kJ m^{-2} day^{-1})	Directly affects photosynthesis
Solar radiation flux to the ground (KW m^{-2} day^{-1})	Dictates fuel moistures, duff moisture, understory response
Photon flux density in PAR (Umol m^{-2})	Incident photon flux density of photosynthetically active radiation
Days since last snow (days)	Good index of time that snow is on the ground
Days since last rain (days)	Index of precipitation environment
Degree-days (°C)	Reflects heat load at a stand
	WXFIRE ecosystem variables
Potential evapotranspiration (kg H_2O yr^{-1})	Potential evaporation and transpiration if no deficiency of water in the soil
Actual evapotranspiration (kg H_2O yr^{-1})	Water actually lost from plant surface due to evaporation and transpiration
Leaf-scale stomatal conductance (M sec^{-1})	Indicates how often stomates are open during the year
Leaf conductance to sensible heat (M sec^{-1})	Ability of foliage to transpire water
Canopy conductance to sensible heat (M sec^{-1})	Ability of canopy to transpire water
Soil water fraction (index)	Indicates amount of water available for plant growth
Water potential of soil and leaves (-MPa)	How tightly leaf holds moisture--high value indicates plant may be water stressed
Volumetric water content (Scalar)	Indicates soil moisture availability
Growing season water stress (-MPa)	Reflects extent of soil drying during the year
Maximum annual leaf water potential (-MPa)	Soil water availability and evapotranspiration
Snowfall (kg H_2O m^{-2} day^{-1})	Amount of snowfall aids in water balance for site
Soil water lost to runoff and ground (kg H_2O m^{-2} day^{-1})	Water that is not stored on-site for plant growth
Soil water transpired by canopy (kg H_2O m^{-2} day^{-1})	Amount of water lost from plants through their stomata by transpiration
Evaporation (kg H_2O m^{-2} day^{-1})	Indicates loss of water other than evapotranspiration
NFDRS - 1-hr wood moisture content (%)	Illustrates fine fuel moisture regime
NFDRS - 10-hr wood moisture content (%)	Illustrates large fuel moisture regime
Keetch-Byram Drought Index	Represents net effect of evapotranspiration and precipitation to produce cumulative moisture deficiency in deep duff and upper soil layers
	Additional terrain and soils data
Elevation (m)	Indirectly affects plant response to climate
Aspect (degrees)	Indirectly affects radiation, water, temperature
Slope (percent)	Indirectly affects soil water, radiation
Landform	Indirectly affects water storage
Topographic relative moisture index	Index reflecting ability of site to hold water
Topographic position index	Index describing topographic setting
Soil depth (cm)	Affects soil water availability

Table 7—Mean, standard deviation, minimum, and maximum values for biophysical gradients in mapping zones 16 and 19.

	Zone 16				Zone 19			
Parameters	**Mean**	**Std dev.**	**Min.**	**Max.**	**Mean**	**Std dev.**	**Min.**	**Max.**
Daily max. temperature (°C)	12.82	3.22	1.76	25.59	10.51	2.46	0.13	15.73
Daily min. temperature (°C)	–2.34	2.51	–11.99	7.95	–3.24	2.02	–12.13	1.96
Daily precipitation (cm)	58.12	20.45	19.49	234.12	64.24	30.32	20.05	282.96
Daily ave. temperature (°C)	5.24	2.82	–5.11	16.72	3.64	2.17	–5.39	8.46
Daily ave. daytime temperature (°C)	8.65	2.99	–2.02	20.69	6.73	2.28	–2.80	11.56
Daily ave. nighttime temperature (°C)	3.15	2.72	–7.00	14.31	1.75	2.11	–7.08	6.66
Daily ave. soil temperature (°C)	0.48	0.26	–0.46	1.52	0.33	0.20	–0.49	0.77
Relative humidity (%)	58.75	2.46	51.91	94.42	61.86	2.74	0.00	72.36
Total solar radiation (kJ m^{-2} day^{-1})	1,181.93	232.14	68.12	1,300.00	1,275.34	115.69	24.60	1,300.00
Solar radiation flux to the ground (KW m^{-2} day^{-1})	67.57	47.62	1.45	178.41	77.67	38.12	0.49	148.14
Photo flux density (Umol m^{-2})	2,426.40	403.88	154.97	2,600.00	2,563.84	197.05	0.00	2,600.00
Days since snowfall (days)	0.91	0.05	0.77	1.00	0.89	0.05	0.69	0.98
Days since rain (days)	1.43	0.17	0.92	1.86	1.32	0.12	0.00	1.63
Degree-days (°C)	2,985.47	819.01	586.67	6,831.58	2,544.67	567.04	641.29	3,878.23
Potential evaporation (kg H_2O yr^{-1})	1,478.25	166.85	434.12	1,997.15	1,120.80	164.02	0.00	1,563.33
Actual evapotranspiration (kg H_2O yr^{-1})	533.67	175.54	147.75	1,852.90	555.52	136.84	0.00	1,646.15
Leaf-scale stomatal conductance (M sec^{-1})	1,199.61	985.41	258.63	12,000.00	2,673.45	2,858.55	0.00	12,000.00
Leaf conductance to sensible heat (M sec^{-1})	9.31	0.36	7.90	10.34	16.43	10.42	9.02	96.40
Canopy conductance to sensible heat (M sec^{-1})	5.60	5.37	1.16	20.65	19.41	17.30	1.56	192.77
Soil water fraction (index)	0.38	0.09	0.04	0.86	0.30	0.16	0.00	0.89
Water potential of soil and leaves (-MPa)	–2.66	1.32	–9.82	–0.01	–4.57	2.58	–9.99	–0.01
Volumetric water content of soil (Scalar)	0.17	0.04	0.02	0.41	0.13	0.07	0.00	0.43
Growing season water stress (-MPa)	–165.70	124.58	–560.00	–0.38	–146.64	160.54	–560.00	–0.19
Maximum annual leaf water potential (-MPa)	–9.62	1.37	–10.00	–0.17	–9.50	1.84	–10.00	–0.10
Snowfall (kg H_2O m^{-2} day^{-1})	0.83	0.53	0.00	5.16	0.83	0.70	0.07	7.10
Soil water lost to runoff and groundwater (kg H_2O m^{-2} day^{-1})	0.18	0.30	0.00	5.57	0.38	0.64	0.00	29.74
Soil water transpired by canopy (kg H_2O m^{-2} day^{-1})	0.91	0.50	0.04	4.62	0.32	0.28	–27.69	3.27
Evaporation (kg H_2O m^{-2} day^{-1})	0.55	0.09	0.06	1.13	1.20	0.22	0.12	2.12
1-hour wood moisture content (%)	16.69	3.50	11.47	100.00	17.88	3.02	12.40	35.00
10-hour wood moisture content (%)	18.37	3.27	12.84	100.00	15.95	3.52	11.41	35.00
Keetch-Byram Drought Index	70.27	48.11	1.83	800.00	45.17	26.89	2.66	255.33

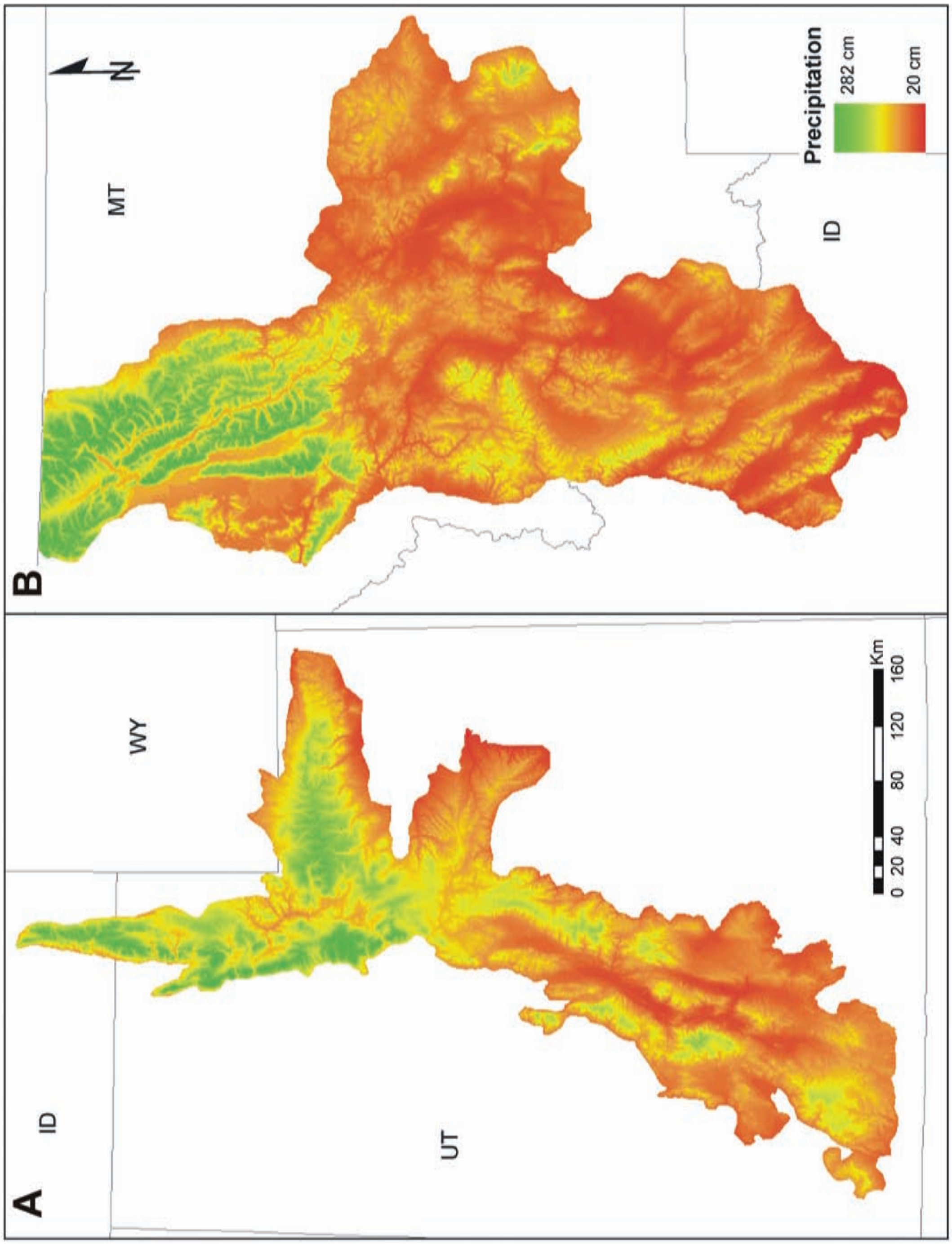

Figure 4—Average annual precipitation (cm) as simulated by WXFIRE for mapping zones 16 and 19.

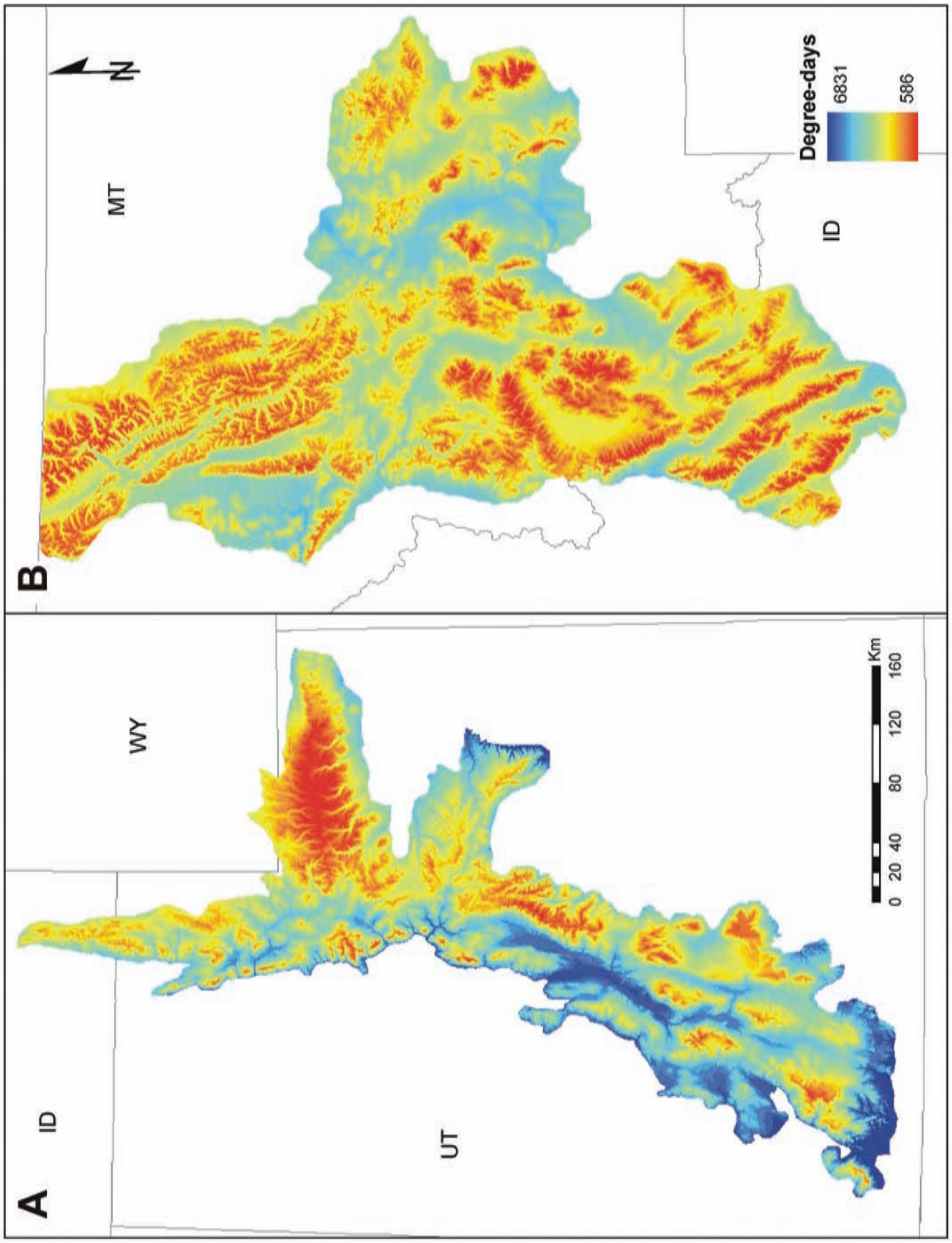

Figure 5—Degree-days (describing heat load of stand) as predicted by WXFIRE for mapping zones 16 and 19.

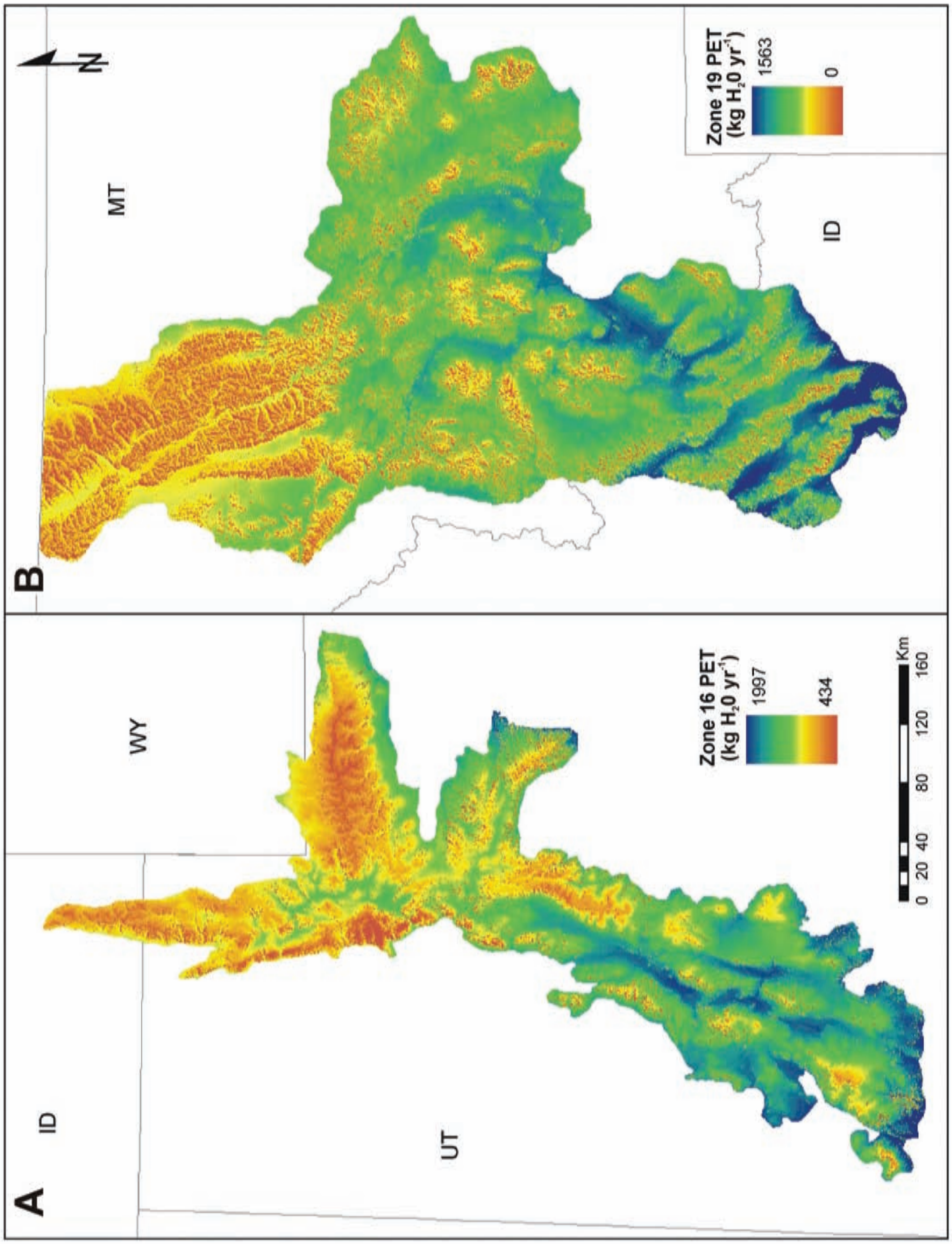

Figure 6—Potential evapotranspiration as predicted by WXFIRE for mapping zones 16 and 19.

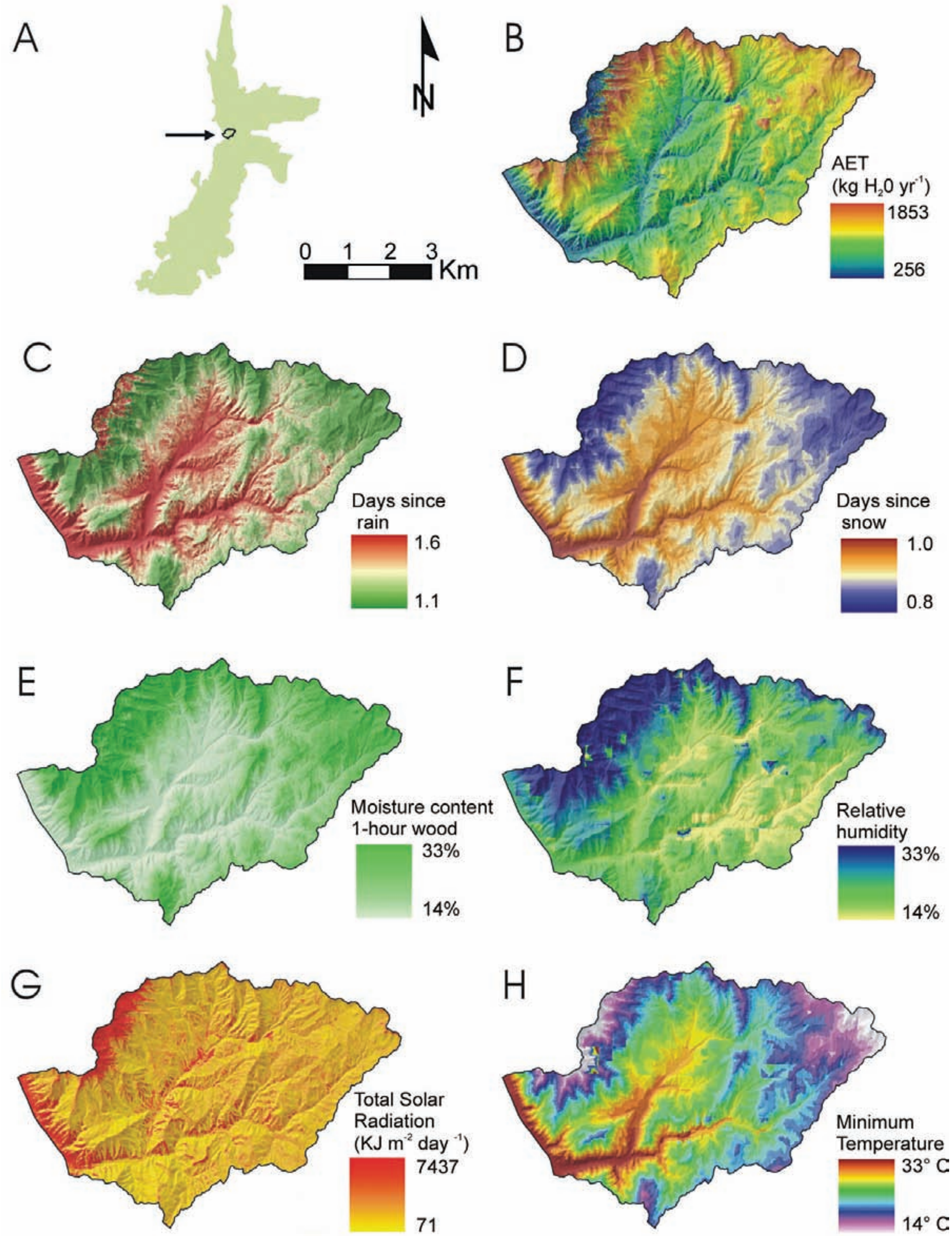

Figure 7—Higher resolution view of key WXFIRE layers used in predicting PVT for forested areas of Zone 16: (A) Zone 16 showing watershed of interest; (B) actual evapotranspiration; (C) days since rain; (D) days since snow; (E) moisture content of 1-hour wood; (F) relative humidity; (G) total solar radiation; and (H) minimum temperature.

landscapes in the two prototype mapping zones. They found that these biophysical gradients had a high level of precision but lacked a high degree of accuracy. WXFIRE model predictions were limited most by the difficulty of accurately quantifying the simulation units and site parameters due to the low quality and consistency of available GIS layers (Keane and Holsinger 2006).

The quality of biophysical gradient data was also constrained by the interpolation of weather data by the DAYMET model and by the integration of that weather data into biophysical gradient estimates. The WXFIRE model relies strongly on predictions of the DAYMET weather model. The DAYMET model offers extensive weather data for the conterminous United States at a high mapping resolution; however, it has limited spatial accuracy and temporal depth (Thornton and others 1997). In many parts of the country, weather stations are scarce, and this sparse distribution reduces the DAYMET model's ability to accurately interpolate weather between stations. In addition, the DAYMET data set spans 18 years (1980-1997), which, although substantial, is relatively short for generalizing the variability in weather patterns over time. For example, if our weather data set extended back one hundred years, we would have data from the drought years of the 1930s and relatively wet years of the 1950s. If such an extensive climate data set were available, spatial variability would likely be different in our suite of biophysical gradient layers—particularly for parameters calculated using non-linear equations, such as actual evapotranspiration (Keane and Holsinger 2006). An 18-year period possibly captured the range of variability in weather for some locations, but in other areas, this narrow time window may reflect only a relatively homogenous weather period, missing the full magnitude of variability.

Additionally, the WXFIRE model calculates weather outputs as annual averages (in other words, data were summed across daily values in a year and averaged across 18 years), which was not the ideal approach for predicting plant species distribution. Plant phenology most closely corresponds to seasonal or daily changes in weather conditions (White and others 2000), not annual time periods. However, the appropriate seasonal or daily time frames that affect vegetation dynamics will vary across regional landscapes. For example, the primary growing season of whitebark pine in alpine habitats ranges from approximately July to October, while sagebrush communities, on average, range from April to October. We used annual time period to capture the potential range of all plant species in a mapping zone; however, with weather data generalized to the coarser annual time frame, the resulting biophysical gradients were less robust for predicting vegetation distributions.

Another limitation in the development of the biophysical gradients for the LANDFIRE Prototype Project is related to the issue of scale, both in terms of spatial resolution and attribute measurement resolution. Our goal was to produce moderate resolution spatial data, which for the biophysical data layers, corresponds roughly to a 30-m resolution. The biophysical gradient layers produced for mapping zones 16 and 19 had a pixel size of 30-m, but the actual spatial resolution of the simulated data was much coarser. The reduced spatial resolution was a result of the limited availability of high resolution input layers for WXFIRE and limited computer resources. We chose only those geospatial data sources that were complete and contiguous across the conterminous United States. The base data layers used to create the WXFIRE input files had a wide variety of spatial resolutions and mapping scales. Weather and soil texture data for the nation were available only at spatial resolutions greater than 30-m. Other input layers were available at a 30-m resolution (for example, topographic data) but could not be fully utilized because we lacked the computer resources to execute model simulations for the large amount of records created at these fine resolutions. Consequently, we classified our finer-scale data layers to broader ranges in their measurement increments leading to coarser attribute measurement resolution. We also assumed that ecophysicological sites were homogenous across broad landscapes and thereby omitted smaller patches in the gradient patterns, decreasing spatial resolution. Moreover, WXFIRE was constructed, for lack of alternatives, under the assumption that the ecophysiological parameters match the simulation units in spatial and temporal scale (Keane and Holsinger 2006), which is rarely true. For example, maximum canopy conductance derived from the ecophysiological site layer has a significantly coarser resolution than terrain-related data.

The true resolution of these biophysical gradient layers was difficult to determine for several reasons. First, the core data layers that were used as input to the WXFIRE model were of varying resolution. Second, the WXFIRE model integrated multiple algorithms and equations for calculation of each biophysical gradient layer. Third, WXFIRE required additional ecophysiological site parameters for simulation—also at varying resolutions. We can illustrate the difficulty in assessing resolution from these compounding influences with the example of potential evapotranspiration (kg H_2O yr^{-1}) calculation. Calculations of potential evapotranspiration required data from six input layers: DAYMET weather, elevation, aspect, slope, ecophysiological site (albedo and others, see Keane and Holsinger 2006), and topographic shading (table 8). The original resolution of these input layers ranged from 30 m to 1 km, although the terrain-related layers (elevation, aspect, slope, and topographic shading) were classified to coarser attribute measurement resolutions (table 5). Actual simulation of potential evapotranspiration involved calculating several variables as inputs to a complex algorithm, and these variables represent processes which introduce additional modifications to data resolution. Specifically, weather data were interpolated from stations across the mapping zone in the DAYMET weather database. These weather data were also scaled down from 1-km data to the simulation unit, and the extent of scaling varied depending on size of the simulation unit. Finally, the actual algorithm to calculate potential evapotranspiration required the input of ecophysiological parameters of varying scale. For example, the ecophysiological parameter albedo can vary over small distances in real landscapes and over short time spans as species change due to phenology. However, we mapped albedo over large areas for broad categories of vegetation types that were considered static instead of dynamic. Overall, the resulting spatial resolution of the potential evapotranspiration layer depended on the integration of all the multiple data inputs and individual processing steps. Perhaps the best method for assessing data resolution would be through accuracy assessments using field-based data. However, observed data for potential evapotranspiration and other ecosystem, weather, and climate WXFIRE variables were not available. The effect of data resolution could also be assessed using sensitivity analysis such as Monte Carlo simulation, and such analyses would be worthwhile to perform in the future. In an effort to inform some understanding of the scale of the data layers, we have presented the data inputs required for modeling each of the biophysical gradients (table 8), the associated data resolution or scale for these input layers (table 2), and the classification scheme of input layers (table 5).

Recommendations for National Implementation

Many of the decisions made in the LANDFIRE Prototype Project aimed to minimize computation time while maintaining information content. Without constraints, it would be ideal to model each 30-m pixel on the landscape. For the LANDFIRE Prototype, however, that would have been intractable due to limited resources, the number of processes required, and narrow time-frames. For instance, we classified input layers and grouped pixels with similar values to create broad simulation units so that the model could be run one time and the outputs applied to many pixels. The overall scheme of this classification and creation of unique simulation units was sufficient, but the details implemented contained some flaws, such as in the soil depth layer's derivation and the DAYMET weather grid inclusion for creating simulation units. We suggest making changes to various phases of the biophysical gradients creation process to increase the quality of output while working within the general simulation framework developed during the LANDFIRE Prototype Project.

Improving Simulation Models

Early in the LANDFIRE Prototype Project, we explored using an ecosystem process model called LF-BGC, in addition to the WXFIRE simulation model (Thornton 1998). LF-BGC is a version of Biome-BGC adapted for the LANDFIRE Project that simulates carbon, water, and nitrogen fluxes to simulate a set of carbon budget metrics and ecophysiological characteristics. The version of LF-BGC available for the LANDFIRE Prototype Project, however, was designed primarily to produce biophysical gradient layers at a 1-km resolution, based on the scale objectives of Biome-BGC. We attempted to create higher-resolution biophysical gradient layers (30 m) by using higher-resolution inputs but discovered that more sophisticated model modifications were needed. A subsequent version of the LF-BGC model was developed that successfully creates higher-resolution biophysical gradient layers. Due to time constraints, however, we were unable to develop the layers with this new version. For the national implementation of LANDFIRE, we recommend incorporating the LF-BGC model to develop a more extensive set of biophysical gradient layers.

The LF-BGC and WXFIRE simulation models have many similarities, including file input, processing, and biophysical gradient output, and we suggest that the two models be combined into a single model executable for the national implementation of LANDFIRE. A number of factors should make this combination straightforward and a logical step towards optimizing model efficiency. First, both LF-BGC and WXFIRE are written in the C+ programming language and contain many equivalent calculations. Second, LF-BGC and WXFIRE have similar required inputs, differing in that WXFIRE requires more physical site information: slope, aspect, and hillshade. These three variables predominantly control the scaling of incoming radiation and its derivatives. Third, both models extract DAYMET weather data—the most time-consuming and process-intensive

Table 8—Data inputs used by WXFIRE to model each of the biophysical gradients. Note: units for each of the biophysical gradient variables are provided in table 7. Diamonds indicate that the input variable was applied in the calculation of the WXFIRE output variable.

WXFIRE variable	DAYMET	Elevation	Aspect	Slope	Soil depth	Soil texture	LAI	Site	Topo. shading
Soil water transpired by canopy	◆	◆	◆	◆	◆	◆		◆	◆
Soil water fraction	◆	◆	◆	◆	◆	◆		◆	◆
Daily maximum temperature	◆	◆							
Daily precipitation	◆	◆					◆	◆	
Daily minimum temperature	◆	◆							
Relative humidity	◆								
Daily average temperature	◆	◆							
Daily average soil temperature	◆	◆							
Daily average daytime temperature	◆	◆							
Daily average nighttime temperature	◆	◆							
Corrected average daily radiation	◆		◆	◆				◆	◆
Shortwave radiation	◆		◆	◆			◆	◆	◆
Photo flux density	◆		◆	◆			◆	◆	◆
Days since snowfall	◆	◆					◆	◆	
Days since rain	◆	◆					◆	◆	
Potential evapotranspiration	◆	◆	◆	◆				◆	◆
Actual evapotranspiration	◆	◆	◆	◆	◆	◆	◆	◆	◆
Degree-days	◆	◆							
Leaf-scale stomatal conductance	◆	◆	◆	◆	◆	◆		◆	◆
Leaf conductance to sensible heat	◆	◆	◆	◆	◆	◆		◆	◆
Canopy conductance to sensible heat	◆	◆	◆	◆	◆	◆		◆	◆
Volumetric water content of soil	◆	◆	◆	◆	◆	◆	◆	◆	◆
Growing season water stress	◆	◆	◆	◆	◆	◆	◆	◆	◆
Water potential of soil and leaves	◆	◆	◆	◆	◆	◆	◆	◆	◆
Maximum annual leaf water potential	◆	◆	◆	◆	◆	◆	◆	◆	◆
Snowfall	◆	◆							
Soil water lost to runoff & groundwater	◆	◆	◆	◆	◆	◆	◆	◆	◆
Evaporation	◆	◆	◆	◆	◆	◆	◆	◆	◆
1-hour wood moisture content	◆	◆	◆	◆				◆	
10-hour wood moisture content	◆	◆	◆	◆				◆	
Keetch-Byram Drought Index	◆								

step for executing either model. If the two models were combined, this call to DAYMET would only occur once. Fourth, the ecosystem variables (see table 6) calculated in WXFIRE are dependent on a site file and LAI data that both represent current land cover. The same (and more) ecosystem variables are output from LF-BGC, and, by combining models, we would no longer require current land cover information.

The process of combining WXFIRE and LF-BGC should be relatively seamless and significantly improve model outputs and efficiency. The unique variables output by WXFIRE, namely the climate derivatives, can readily be added to the LF-BGC model. This procedure can be done with minimal change to the core LF-BGC program and without affecting the stand-alone output. This proposed combination of the models would remove a major source of problems and error and virtually cut simulation times and computing resource needs in half.

In addition to combining the models, we suggest a change in the way that LF-BGC is parameterized and executed. During exploratory simulations, LF-BGC was run with the evergreen needle leaf forest plant functional type (PFT) across simulation units in Zone 16. Our goal in using this model was not to calculate the actual net primary productivity (NPP), but to represent the relative differences in potential NPP across landscapes in order to delineate unique biophysical settings. We chose to simulate the PFT with the narrowest ecological amplitude to maximize the information content of the output and selected only one to remain within our deadlines. This logic could be applied for most areas of the U.S.; however, some landscapes may exist that cannot sustain an evergreen needle leaf PFT. Sole use of the evergreen needle leaf PFT for LF-BGC simulations does not provide enough information to distinguish unique biophysical settings in such landscapes. Assuming that efficiency is improved and resources are increased for the national effort, we suggest adding the C3 grass (cool season) PFT to the simulation protocol. By modeling the two plant functional types with the narrowest (evergreen needle leaf) and broadest (C3 grass) ecological amplitudes, we can achieve a more complete picture of the biophysical gradients that exist across the entire United States.

Improving Model Input Layers

To minimize the number of unique simulation units, we classified much of the input data to broad categories. Classification served to minimize the number of simulations while attempting to remain within the bounds of model sensitivity. We propose a number of changes to the methods for creating the input layers used to create simulation units.

We derived soil depth from STATSGO slope groups that were further divided with a topographic convergence index (TCI). The derived soil depth layer showed a very speckled pattern or *pixelation* and contained a definite footprint of the hydrologic modeling that carried through to final biophysical gradient layers in the form of linear hydrologic features. Further examination determined that the pixelation of the soil depth layers was the dominant determinate of the size and shape of simulation units. This pattern was due largely to characteristics of the soil depth layer that were undesirable. The input of flow accumulation to the soil depth derivation process resulted in long, linear artifacts in the simulation units resulting from limitations in the flow direction grid. We explored different flow direction layers of varying complexity, but all created the same artifacts in the final layers. The multiple flow direction layers, in addition to the high degree of pixelation in the depth values, reduced our confidence in the derived soil depth values. We recommend eliminating the TCI soil depth calculation and using the soil depth information taken directly from STATSGO but modified by slope group, as with the soil texture information. In addition, we recommend exploring techniques to modify the soil depth estimation according to the coarse fragment proportion.

Reducing the soil depth layer complexity would provide the flexibility to increase the number of categories in our other model input layers and thereby improve the characterization of ecologically important and unique physical patches on the landscape for creating simulation units. We advocate increasing the number of classes in the terrain-related layers as follows:

- **Aspect**—Divide into eight classes: north 338 – 22, northeast 23 – 67, east 68 – 112, southeast 113 – 157, south 158 – 202, southwest 203 – 247, west 248 – 292, and northwest 293 – 337.
- **Slope**—Divide into five classes: <4 percent, 5 – 14 percent, 15 – 29 percent, 30 – 79 percent, and 80 – maximum percent.
- **Hillshade**—Divide (as a value between 0 and 1) into ten classes with the maximum class value representing each class (in other words, 0.1, 0.2, and so forth).

As in the prototype effort, the value assigned to the pixel should be the midpoint of the class range for aspect and slope.

We also propose a change in the extraction and handling of the DAYMET weather data. For the LANDFIRE Prototype Project, the center coordinates of 1-km DAYMET pixels were used to create simulation units and to extract weather data for each simulation unit within a 1-km pixel. A lapse rate was applied based on the elevation difference between the simulation unit and DAYMET pixel. A significant 1-km artifact of this DAYMET grid remained in many output layers, even when various smoothing techniques were implemented. We propose removing the DAYMET grid from the suite of layers used to create simulation units and employing a more sophisticated smoothing process to scale the weather data down to better represent our 30-m simulation units Specifically, we suggest applying a lapse rate based on bilinear interpolation to the four surrounding DAYMET pixels closest to the center coordinates for each simulation unit.

The ecophysiological site and LAI data layers were created based on current land use and land cover data, and these layers were used to determine unique simulation units for developing the biophysical gradient layers. When the site and LAI layers were used to create simulation units, they not only generated artifacts but had no bearing on biophysical attributes that define environmental site potential or biophysical setting. For these reasons, we recommend omitting these layers in the creation of unique simulation units. In combining the WXFIRE and LF-BGC models, the ecophysiological site and LAI inputs could be eliminated because they are inherent to the BGC PFT parameterization and will represent more generic potential rather than current land use and land cover.

Improving Simulation Unit Development

We propose some changes to the protocol for defining the simulation units with respect to reducing data volume and increasing simulation efficiency. We identified three major limitations in our methods, the removal of which would improve the quality of the simulation units. First, as stated in the previous section, the ecophysiological site, LAI, and the 1-km DAYMET layers should not be used to create simulation units. These layers impose artificial footprints and are not physical features that affect the biophysical potential of a landscape patch. Second, by removing the DAYMET grid as a controlling factor in creating simulation units, we can maintain the data at its native resolution rather than re-sampling all data to 25 m. Following these two changes to the input data used to create simulation units, we propose changes in the delineation methods aimed towards reducing the overall number of simulation units through classification and combination of the input layers.

In our proposed method for creating simulation units, we first assume that the following: First, executing the model to create biophysical gradient layers for each 30-m pixel is computationally problematic. Second, model input layers can be classified within the bounds of model sensitivity, thereby decreasing data volume without losing information. Third, physical limits—regarding the size of the simulation units—can be imposed without losing desired spatial detail. We suggest first combining the following input layers with new class definitions: elevation, slope, aspect, hillshade, soil depth, and soil texture (sand, silt, and clay). This combination would assign a unique identification number to each unique combination of the variables. We then suggest grouping adjacent like pixels based on the combined output. This aggregation would separate any pixels that have the same biophysical gradient properties but are separated in geographic space. We then propose applying a minimum mapping unit of ~1 ha to these simulation units to reduce the total number. Because the DAYMET weather data is interpolated to scale it to the 30-m DEM, a maximum size for simulation units should be imposed, such that the units are less than 1 km; we propose using a maximum axis length of 750 m. This set of steps represents small changes, but it would result in a significant reduction in the number of simulation units. Additionally, we expect that the gain in biophysical information through these new methods would significantly improve the quality of the output biophysical gradient layers.

Conclusion

Integration of remote sensing, simulation modeling, and gradient analysis proved to be an efficient and successful approach for mapping broad-scale vegetation, wildland fuel, and fire regime characteristics in the LANDFIRE Prototype Project. The ability of remote sensing and ecosystem simulation to portray spatial distributions of biophysical gradients enables the efficient construction of reasonably accurate maps that are critical for both fire managers and ecologists. While there were a variety of limitations encountered during the application of the LANDFIRE Prototype Project biophysical gradient modeling approach, the lessons learned will prove valuable when LANDFIRE methods are applied across the entire United States.

For further project information, please visit the LANDFIRE website at www.landfire.gov.

The Authors

Lisa Holsinger is a GIS Specialist with the USDA Forest Service, Rocky Mountain Research Station, Missoula Fire Sciences Laboratory (MFSL). Holsinger joined the MFSL in 2002 and has worked on developing and analyzing spatial data for simulation models applied to large landscapes. She has developed GIS data and input for the WXFIRE and LANDSUM simulation models and HRVStat program, run simulations, and produced associated spatial data. She has also conducted sensitivity analyses for both the WXFIRE and LANDSUM models. Prior to the Fire Sciences Laboratory, she worked as a Fisheries Biologist and GIS Specialist for the National Marine Fisheries Service conducting research and management for the conservation of west coast salmon populations. Holsinger received her B.S. degree in Biological Sciences from University of California, Davis in 1984 and her M.S. degree in Fisheries at the University of Washington in 1988.

Robert E. Keane is a Research Ecologist with the USDA Forest Service, Rocky Mountain Research Station, Missoula Fire Sciences Laboratory (MFSL). Since 1985, Keane has developed various ecological computer models for the Fire Effects Project for research and management applications. His most recent research includes the development of a first-order fire effects model, construction of mechanistic ecosystem process models that integrate fire behavior and fire effects into succession simulation, restoration of whitebark pine in the Northern Rocky Mountains, spatial simulation of successional communities on landscapes using GIS and satellite imagery, and the mapping of fuels for fire behavior prediction. He received his B.S. degree in Forest Engineering in 1978 from the University of Maine, Orono, his M.S. degree in Forest Ecology in 1985 from the University of Montana, and his Ph.D. degree in Forest Ecology in 1994 from the University of Idaho.

Russell Parsons is a GIS Specialist with the USDA Forest Service, Rocky Mountain Research Station, Missoula Fire Sciences Laboratory (MFSL). Parsons has worked in GIS and remote sensing since 1997. He received his B.S. degree in Forestry in 1992 from the University of California, Berkeley, and his M.S. degree in 1999 in Forest Resources from the University of Idaho. He is currently earning his Ph.D. at the University of Montana's School of Forestry. Parsons previously worked as a fire monitor in California's Sequoia and Kings Canyon national parks, and served as an agroforestry extensionist volunteer in the Peace Corps in Ecuador from 1995 to 1997.

Eva Karau is a GIS Specialist with the USDA Forest Service, Rocky Mountain Research Station, Missoula Fire Sciences Laboratory (MFSL). She has worked for the Fire Effects Research Unit on various projects involving GIS analysis, remote sensing, field sampling, and fire effects modeling. She received her B.A. in Geology from the University of Montana in 1995 and her M.S. in Forestry from the University of Montana in 2002.

Acknowledgments

We would like to thank the USDA Forest Service Fire and Aviation Management Washington Office for funding the LANDFIRE Prototype Project. We thank Dr. Janet Ohmann of the USDA Forest Service Pacific Northwest Research Station, Jeff Jones of the USDA Forest Service Flathead National Forest, and Alisa Keyser, Maureen Mislivets, and Dr. Matthew Rollins at the Missoula Fire Sciences Laboratory for their technical review and thoughtful comments on the manuscript. We also thank Sarah Pratt and Don Long at the Missoula Fire Sciences Laboratory, Dr. Peter Thornton at Colorado State University, and Dr. Norman Bliss, Zheng Zhang, and Dr. Zhiliang Zhu at the USGS Center for Earth Resources Observation and Science for their technical input and valuable assistance in this project. Finally, we thank Christine Frame of Systems for Environmental Management for technical editing and Dennis Simmerman of the Missoula Fire Sciences Laboratory for graphic design.

References

Arno, S.F.; Simmerman, D.G.; Keane, R.E. 1985. Forest succession on four habitat types in western Montana. Gen. Tech. Rep. INT_GTR-177. Ogden, UT: U.S. Department of Agriculture, Forest Service, Intermountain Forest and Range Experiment Station.

Austin, M.P. 1980. Searching for a model for vegetation analysis. Vegetatio. 45:11-21.

Austin, M.P. 1985. Continuum concept, ordination methods, and niche theory. Anuual Review of Ecology and Systematics. 16:39-61.

Austin, M.P.; Smith, T.M. 1989. A theory of spatial and temporal dynamics in plant communities. Vegetatio. 83:49-69.

Beven, K.J.; Kirkby, M.J. 1979. Towards a simple, physically based, variable contributing aera model of catchment hydrology. Bulletin of the International Association of Hydrological Science. 24:43-69.

Burrough, P.A. 1986. Principles of Geographical Information Systems for Land Resources Assessment. New York, NY: Oxford University Press. 50 p.

ESRI 2002. Arc/Info 8.3 Software. Redlands, CA: Environmental Systems Research Institute.

Franklin, J. 1995. Predictive vegetation mapping: geographic modeling of biospatial patterns in relation to environmental gradients. Prog. Phys. Geogr. 19:474-499.

Gosz, J.R. 1992. Gradient analysis of ecological change in time and space: Implications for forest management. Ecological Applications. 2(3): 248-261.

Guisan, A.; Zimmerman, N.E. 2000. Predictive habitat distribution models in ecology. Ecological Modeling. 135:147-186.

Haplin, P. N. 1999. GIS Analysis for Conservation Site Design: A short-course developed for the Nature Conservance. Raleigh, NC: Nicholas School of the Environment-Landscape Ecology Lab, Duke University.

Hessl, A. E.; Milesi, C; White, M.A.; Peterson, D.L.; Keane, R.E. 2004. Ecophysiological parameters for Pacific Northwest trees. Gen. Tech. Rep. PNW-GTR-618, Portland, OR: U.S. Department of Agriculture, Forest Service, Pacific Northwest Research Station.

Jenson, S. K.; Domingue, J.O. 1988. Extracting Topographic Structure from Digital Elevation Data for Geographic Information System Analysis. Photogrammetric Engineering and Remote Sensing. 54(11): 1593-1600.

Keane, R.E.; Rollins, M.G.; McNicoll, C.H.; Parsons, R.A. 2002. Integrating ecosystem sampling, gradient modeling, remote sensing, and ecosystem simulation to create spatially explicit landscape inventories. Gen. Tech. Rep. RMRS-GTR-92. Fort Collins, CO: U.S. Department of Agriculture, Forest Service, Rocky Mountain Research Station, 61 p.

Keane, R.E.; Holsinger, L. 2006. Simulating biophysical environment for gradient modeling and ecosystem mapping using the WXFIRE program: Model documentation and application. Gen. Tech. Rep. RMRS-GTR-168DVD. Fort Collins, CO: U.S. Department of Agriculture, Forest Service, Rocky Mountain Research Station. 61 p. [Online]. Available: http://www.fs.fed.us/rm/pubs/rmrs_gtr168.html [May 18, 2006].

Kessell, S. R. 1976. Wildland inventories and fire modeling by gradient analysis in Glacier National Park. In: Proceedings of the Tall Timbers Fire Ecology Conference and Fire and Land Management Symposium. Tallahassee, FL: Tall Timbers Research Station. Pp. 115-162.

Kessell, S. R. 1979. Gradient modeling: resource and fire management. New York, NY: Springer-Verlag.

Korol, R. L. 2001. Physiological attributes of eleven Northwest conifer species. Gen. Tech. Rep. RMRS-GTR-73. Fort Collins, CO: U.S. Department of Agriculture, Forest Service, Rocky Mountain Research Station.

Natural Resources Conservation Service. 1995a. State soil geographic data base (STATSGO): Data user's guide. Miscellaneous Publication Number 1492. Washington D.C.: U.S. Department of Agriculture, Natural Resources Conservation Service, National Soil Survey Center.

Natural Resources Conservation Service. 1995b. Soil survey geographic (SSURGO) data base, data use information. Miscellaneous Publication Number 1527. Washington D.C.: U.S. Department of Agriculture, Natural Resources Conservation Service, National Soil Survey Center.

Nemani, R.; Pierce, L.; Running, S.; Bank, L. 1993. Forest ecosystem processes at the watershed scale: sensitivity to remotely-sensed leaf area index estimates. International Journal of Remote Sensing. 14(13):2519-2534.

Neufeldt, V.; Guralnik, D.B., eds. 1988. Webster's New World Dictionary, Third College Edition. New York, NY: Simon & Schuster. 1,574 p.

Ohmann, J.L.; Gregory, M.J. 2002. Predictive mapping of forest composition and structure with direct gradient analysis and neareset neighbor imputation in coastal Oregon, USA. Canadian Journal of Forest Research. 32:725-741.

Parker, A. J. 1982. The Topographic Relative Moisture Index: An Approach to Soil-Moisture in Mountain Terrain. Physical Geography. 3(2): 160-168.

Rollins, M.G.; Keane, R.E.; Parsons, R.A. 2004. Mapping fuels and fire regimes using remote sensing, ecosystem simulation and gradient modeling. Ecological Applications. 14(1): 75-95.

SAS Institute Inc. 2001. SAS OnlineDoc, Version 8. Cary, NC: SAS Institute Inc.

Steele, R.; Geier-Hayes, K. 1989. The Douglas-Fir/Nine-bark habitat type in central Idaho: succession and management. Gen. Tech. Rep. INT-GTR-252. Ogden, UT. U.S. Department of Agriculture, Forest Service, Intermountain Research Station.

Tarboton, D. G.; Bras, R.L.; Rodriguez-Iturbe, I. 1991. On the Extraction of Channel Networks from Digital Elevation Data, Hydrological Processes. Vol. 5: 81-100.

Thornton, Peter E. 1998. Regional ecosystem simulation: Combining surface- and satellite-based observations to study linkages between terrestrial energy and mass budgets. Missoula, MT: University of Montana. 280 p.

Thornton, P.E.; Running, S.W.; White, M.A. 1997. Generating surfaces of daily meteorological variables over large regions of complex terrain. Journal of Hydrology. 190: 214-251.

Thornton, P.E.; Running, S.W. 1999. An improved algorithm for estimating incident daily solar radiation from measurements of temperature, humidity, and precipitation. Agricultural and Forest Meteorology. 93(4): 211-228.

Thornton, P.E.; White, J.D. 2000. Biogeochemical characterization of the Columbia River basin using the BGC model: ecophysiological inputs and landscape descriptions. Final Report on file at Intermountain Fire Sciences Laboratory, Missoula, MT. 28 p.

Thornton, P.E.; Law, B.E.; Gholz, H.L.; Clark, K.L.; Falge, E.; Ellsworth, D.S.; Goldstein, A.H.; Monson, R.K.; Hollinger, D.; Falk, M.; Chen, J.; Sparks, J.P. 2002. Modeling and measuring the effects of disturbance and history and climate on carbon and water budgets in evergreen needle leaf forests. Agricultural and Forest Meteorology. 113: 185-222.

Waring, R.H.; Running, S.W. 1998. Forest Ecosystems: analysis at multiple scales. San Diego, CA: Academic Press.

White, M. A.; Thornton, P.E.; Running, S.W. 1997. A continental phenology model for monitoring vegetation responses to interannual climatic variability. Global Biogeochemical Cycles. 11:217-234.

White, M. A.; Thornton, P.E.; Running, S.W.; Nemani, R. 2000. Parameterization and sensitivity analysis of the Biome-BGC terrestrial ecosystem model: Net primary production controls. Earth Interactions. 4(3): 1-85.

Whittaker, R. H. 1967. Gradient analysis of vegetation. Biological Review. 42: 207-264.

Whittaker, R.H. 1973. Direct gradient analysis. In: Whittaker, R.H., ed. Ordination and classification of communities. The Hague, Netherlands: Dr. W. Junk. Pp. 1-52.

Whittaker, R. H. 1975. Communities and Ecosystems. New York, NY: Macmillan.

Zheng, D.; Hunt, Jr., E.R.; Running, S.W. 1996. Comparison of available soil water capacity estimated from topography and soil series information. Landscape Ecology. 11(1):3-14.

Personal Communications

Bliss, N. 2002. [Telephone communication]. U.S. Geological Service/Eros Data Center, Sioux Falls, South Dakota.

Zheng Zhang. 2002. [File]. SAIC-Geospatial Data Analyst, U.S. Geological Service/Eros Data Center, Sioux Falls, South Dakota. On file at: U.S. Department of Agriculture, Forest Service, Rocky Mountain Research Station, Fire Sciences Laboratory, Missoula, MT.